

Strong uniaxial in-plane magnetic anisotropy of (001)- and (011)-oriented $\text{La}_{0.67}\text{Sr}_{0.33}\text{MnO}_3$ thin films on NdGaO_3 substrates

H. Boschker,^{1,*} M. Mathews,¹ E. P. Houwman,^{1,†} H. Nishikawa,^{1,2} A. Vailionis,³ G. Koster,¹ G. Rijnders,¹ and D. H. A. Blank¹

¹*MESA + Institute for Nanotechnology, University of Twente, 7500 AE Enschede, The Netherlands*

²*B.O.S.T., Kinki University, 930 Nishi-Mitani, Kinokawa 649-6493, Japan*

³*Geballe Laboratory for Advanced Materials, Stanford University, Stanford, California 94305, USA*

(Received 17 December 2008; revised manuscript received 23 April 2009; published 17 June 2009)

Epitaxial $\text{La}_{0.67}\text{Sr}_{0.33}\text{MnO}_3$ (LSMO) ferromagnetic thin films were coherently grown on NdGaO_3 (NGO) substrates with different crystal orientations of the surface plane. On the $(110)_o$ - and $(001)_o$ -oriented substrates, the film grows in the $(001)_{pc}$ orientation, and on the $(100)_o$ -, $(010)_o$ -, and $(112)_o$ -oriented substrates the film is $(011)_{pc}$ oriented (we will use subindices o and pc for the orthorhombic and pseudocubic crystal structures, respectively). The lattice parameters and pseudocube angles of the deformed LSMO pseudocube have been determined from x-ray diffraction measurements. The in-plane magnetic easy and hard directions of these films have been determined from the dependence of the remnant magnetization on the angle of the in-plane applied field. For all substrate orientations there is a strong in-plane uniaxial magnetic anisotropy, determined by the crystal directions of the substrate surface. The easy and hard magnetic-anisotropy directions are explained consistently by the (bulk) inverse magnetostriction model, except for the film on NGO $(112)_o$.

DOI: [10.1103/PhysRevB.79.214425](https://doi.org/10.1103/PhysRevB.79.214425)

PACS number(s): 75.30.Gw, 75.47.Lx, 75.70.Ak

I. INTRODUCTION

The $\text{La}_{1-x}\text{A}_x\text{MnO}_3$ manganites, where A is a divalent alkali earth element ($A=\text{Ba}, \text{Sr}, \text{Ca}$), have been intensively studied, instigated by their observed colossal magnetoresistance (CMR) effects near the ferromagnetic-paramagnetic transition temperature, T_C . $\text{La}_{0.67}\text{Sr}_{0.33}\text{MnO}_3$ (LSMO) is a ferromagnetic half-metal, which is expected to show near 100% polarization of the conduction-electron spin and therefore often used as electrode material in magnetic tunnel junctions (MTJs).¹⁻³

In MTJs the device current is sensitive to the relative orientation of the magnetization vector in the two electrodes. Any deviation from full (anti)parallelism will result in a reduced tunnel magnetoresistance ratio (TMR). The preferential direction of the magnetization in a ferromagnet is determined by the magnetic anisotropy, which includes shape anisotropy, surface anisotropy, and magnetocrystalline anisotropy. For LSMO grown on $(001)_c$ (we will use subindices c, o, and pc for the cubic, orthorhombic, and pseudocubic crystal structures, respectively) SrTiO_3 (STO) different mechanisms compete, such as a uniaxial contribution from the surface steps, the substrate strain-induced biaxial magnetocrystalline anisotropy, and the shape anisotropy.⁴⁻⁶ As was recently pointed out, this competition between the different mechanisms results in nanoscale magnetic-domain formation in these films.⁷ In order to obtain electrodes with a well-defined magnetization direction and abrupt switching behavior, LSMO films with strong uniaxial anisotropy are required.

Apart from the magnetic properties, the surface termination of the electrodes at the interfaces with the barrier of an MTJ is also considered to be of major importance for the MTJ characteristics. In contrast to the $(001)_{pc}$ surface which has a $(\text{MnO}_2)^{d-}$ or $(\text{La}_{0.7}\text{Sr}_{0.3}\text{O})^{d+}$ terminating layer, the $(011)_{pc}$ surface has a $(\text{LaSrMnO})^{4+}$ or a purely $(\text{O}_2)^{4-}$ termi-

nation. For an MTJ with $(011)_{pc}$ interfaces between the electrodes and the barrier material, the top and bottom interfaces are expected to be symmetrical and without interfacial charge transfer.^{8,9}

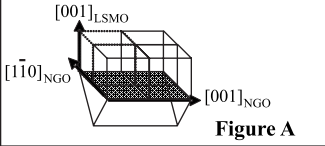
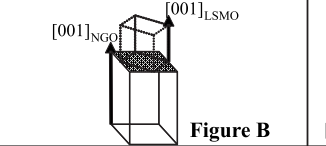
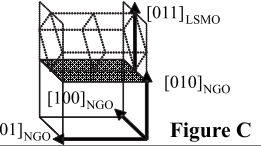
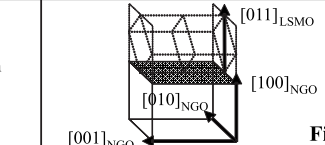
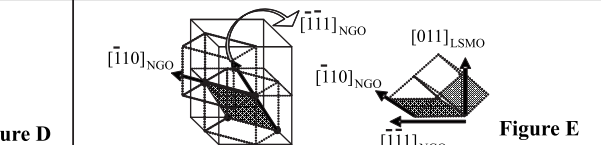
The magnetic properties of LSMO films are known to be very sensitive to the strain imposed by the lattice mismatch between the film and the substrate.¹⁰⁻¹³ Magnetic properties of LSMO thin films are mainly studied in systems with $(001)_{pc}$ -oriented LSMO, which is grown on SrTiO_3 $(001)_c$, NdGaO_3 (NGO) $(110)_o$, and LaAlO_3 (LAO) $(001)_{pc}$. Generally compressive strain (LAO) enhances out-of-plane magnetization, whereas tensile strain (STO) increases the in-plane magnetization component. The NGO $(110)_o$ substrate imposes compressive strain, which competes with the effect of demagnetization, and both out-of-plane¹⁰ and in-plane¹² magnetizations have been observed.

Here, we report on the determination of the in-plane magnetic anisotropy in thin (<50 nm) LSMO films on NGO with different surface crystal planes [NGO $(110)_o$, $(100)_o$, $(010)_o$, $(001)_o$, and NGO $(112)_o$]. LSMO is $(011)_{pc}$ oriented on NGO $(100)_o$, NGO $(010)_o$, and NGO $(112)_o$, and on the other substrates the orientation is $(001)_{pc}$. The different surface-plane orientations of the substrate impose a specific strain on the film which changes the LSMO crystal structure and therefore the magnetocrystalline anisotropy. In all cases the in-plane magnetization shows a strong uniaxial anisotropy. The LSMO pseudocube lattice parameters are determined by x-ray diffraction (XRD) and the easy and hard axis directions are determined by the substrate in-plane crystal directions. In all cases, except for the film on NGO $(112)_o$, the easy axis directions follow from the inverse magnetostriction effect.

II. CRYSTAL STRUCTURE

The orthorhombic crystal structure of NGO (Ref. 14) has lattice parameters $a=5.43$ Å, $b=5.50$ Å, and $c=7.71$ Å.

TABLE I. In-plane and out-of-plane lattice directions for LSMO on NGO with different surface-plane orientations. The lattice mismatch is calculated for the in-plane directions. Figures (A)–(E) show the surface plane of the substrate indicated in gray for the NGO (110)_o, NGO (001)_o, NGO (010)_o, NGO (100)_o, and NGO (112)_o substrates, respectively.

	LSMO(001) _{pc} on NGO(110) _o			LSMO(001) _{pc} on NGO(001) _o			LSMO(011) _{pc} on NGO(010) _o		
	In-plane		Out-of-plane	In-plane		Out-of-plane	In-plane		Out-of-plane
Directions	$[\bar{1}\bar{1}0]_o = [010]_{pc}$	$[001]_o = [100]_{pc}$	$[110]_o = [001]_{pc}$	$[100]_o = [110]_{pc}$	$[010]_o = [\bar{1}\bar{1}0]_{pc}$	$[001]_o = [001]_{pc}$	$[\bar{1}\bar{1}0]_o = [01\bar{1}]_{pc}$	$[001]_o = [110]_{pc}$	$[010]_o = [011]_{pc}$
Lattice mismatch	-0.47%	-0.70%		-1.11%	0.16%		-1.11%	-0.70%	
Growth	 <p style="text-align: center;">Figure A</p>			 <p style="text-align: center;">Figure B</p>			 <p style="text-align: center;">Figure C</p>		
	LSMO(011) _{pc} on NGO(100) _o			LSMO(011) _{pc} on NGO(112) _o					
	In-plane		Out-of-plane	In-plane		Out-of-plane			
Directions	$[010]_o = [0\bar{1}1]_{pc}$	$[001]_o = [100]_{pc}$	$[100]_o = [011]_{pc}$	$[\bar{1}10]_o = [\bar{1}00]_{pc}$	$[\bar{1}\bar{1}1]_o = [0\bar{1}1]_{pc}$	$[111]_o = [011]_{pc}$			
Lattice mismatch	0.16%	-0.70%		-0.47%	-0.59%				
Growth	 <p style="text-align: center;">Figure D</p>			 <p style="text-align: center;">Figure E</p>					

NGO: $a_{NGO} = [100]_o = 0.543\text{nm}$, $b_{NGO} = [010]_o = 0.550\text{nm}$, $c_{NGO} = [001]_o = 0.771\text{nm}$; LSMO: $a_{pc} = 0.388\text{nm}$.

Because the NGO lattice parameters are all different, there are various in-plane strain states possible for the LSMO films, depending on the substrate surface plane orientation. The in-plane lattice mismatch between LSMO and NGO is defined as $m_{[abc]} = (a_{NGO} - a_{LSMO}) / a_{LSMO}$, where a_{LSMO} and a_{NGO} are the lattice constants of the LSMO pseudocube and the NGO substrate, respectively, in the direction $[abc]_o$ of the substrate. The calculated in-plane lattice mismatch for the different orientations of the NGO substrate is given in Table I. The NGO (110)_o substrate orientation results in a (001)_{pc} oriented LSMO film due to the “cube-on-cube” stacking, as shown schematically in figure A in Table I. The in-plane sides of the LSMO pseudocube are aligned along the $[\bar{1}\bar{1}0]_o$ and the $[001]_o$ lattice directions of the NGO substrate. The only other NGO orientation that results in LSMO (001)_{pc} growth is NGO (001)_o. In that case the LSMO cube is rotated in plane over 45° with respect to the NGO $[100]_o$ direction and the pseudocube is in plane aligned along the $[110]_o$ and $[1\bar{1}0]_o$, as is shown in figure B in Table I. The NGO (010)_o (figure C), (100)_o (figure D), and (112)_o (figure E) substrates result in growth in the (011)_{pc} direction of the LSMO, with different values for the lattice mismatch along the two in-plane directions for each substrate orientation (see Table I).

III. EXPERIMENTAL RESULTS

The LSMO thin films (<50 nm) were grown on the NGO substrates of different orientations $[(110)_o, (001)_o, (100)_o,$

$(010)_o,$ and $(112)_o]$ by pulsed laser deposition. The surface treatments necessary for a single terminated surface are described elsewhere.¹⁵ During the deposition material was ablated from a stoichiometric target with a laser fluence of 3 J/cm². The oxygen background pressure was 0.35 mbar and the substrate temperature was 750 °C. The target to substrate distance was fixed at 4 cm. After LSMO deposition, the films were cooled to room temperature at a rate of 10 °C/min in a 1 bar pure oxygen atmosphere. Atomic force microscopy measurements showed smooth surfaces with unit-cell high steps. The step heights were determined to be ~3.9 and ~2.7 Å for LSMO (001)_{pc} and LSMO (011)_{pc}, respectively.

XRD measurements were used to determine the directions of the crystal axes of the NGO substrate and the structure of the LSMO film. The length of the pseudocubic lattice vector in the out-of-plane direction was obtained from XRD θ - 2θ measurements. In comparison with the bulk LSMO value an out-of-plane elongation of the unit cell is found for all surface plane orientations, indicative of the compressive strain in the films. In order to determine the length of the in-plane lattice vectors reciprocal space mapping of an asymmetric reflection has to be performed. Figure 1 shows the reciprocal space maps of a 50 nm film of LSMO grown on NGO (110)_o at the $(260)_o$ $[(024)_{pc}]$, $(620)_o$ $[(0\bar{2}4)_{pc}]$, $(444)_o$ $[(204)_{pc}]$, and $(44\bar{4})_o$ $[(\bar{2}04)_{pc}]$ reflections. All the maps show that the in-plane component of the film peak is equal to that of the substrate indicating coherent growth. For the complete determination of the unit cell not only the lengths but also the angles between the vectors have to be measured. The angle

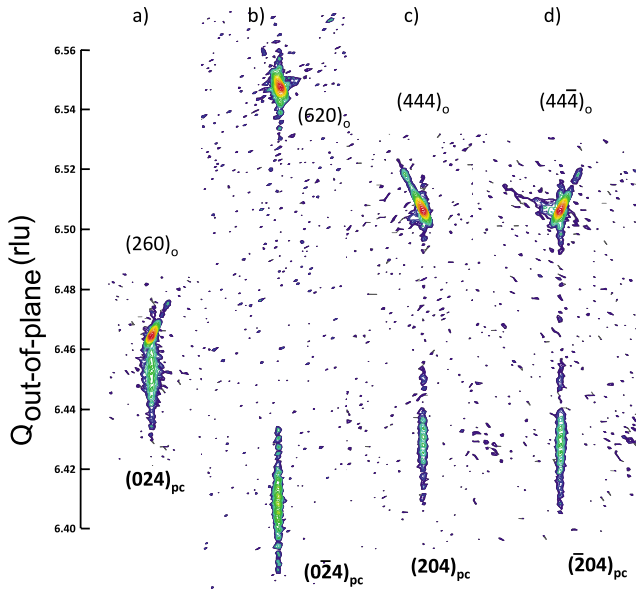


FIG. 1. (Color online) Reciprocal space maps of LSMO grown on NGO (110)_o at (a) the NGO (260)_o, (b) the NGO (620)_o, (c) the NGO (444)_o, and (d) the NGO (444)_o reflections. Here we used $Q = 4\pi \sin \theta / \lambda$, where θ is the Bragg angle and $\lambda = 1.5406 \text{ \AA}$. Q has an out-of-plane component in the (110)_o direction and the in-plane components are in the $[1\bar{1}0]_o$ direction [cases (a) and (b)] and $[001]_o$ direction [cases (c) and (d)]. Indices of the film reflections are shown in bold.

between the two in-plane lattice directions follows from the substrate surface structure. This angle is 90° for LSMO grown on NGO (110)_o, NGO (100)_o, and NGO (010)_o but not for LSMO grown on NGO (001)_o and NGO (112)_o. The angle between an in-plane and the out-of-plane lattice vector can be obtained from the difference in the lattice spacing between an asymmetric reflection with a positive and one with the same negative in-plane contribution.¹⁶ In Fig. 1 [for LSMO on NGO (110)_o] the peaks corresponding to the $(204)_{pc}$ and $(\bar{2}04)_{pc}$ reflections have the same lattice spacing, whereas the peaks corresponding to the $(024)_{pc}$ and $(0\bar{2}4)_{pc}$ reflections have unequal lattice spacing. From this difference an angle α of 89.6° is derived. For LSMO grown on the other four surface-plane orientations of NGO the angles between the in-plane and out-of-plane directions are all 90° . The lengths and angles of the pseudocubic unit cell of LSMO grown on the different surface-plane orientations of NGO are summarized in Table II. The measurements show that all films are fully coherently strained to the substrate surface.

Now the crystal structure of the different films is known, we turn to the magnetic properties. Usually torque measurements are used to determine the easy axis directions and the anisotropy strength. However, such measurements did not provide conclusive information on the anisotropy in the thin films considered here because the torque signal was dominated by the substrate signal.¹⁷ Instead we used vibrating sample magnetometer (VSM) magnetization measurements to determine the easy axis directions.¹⁸ Room-temperature hysteresis loops were measured as a function of the in-plane

field angle, ϕ_H . The loops show the typical features of a uniaxial anisotropy: a square loop in the easy direction and an approximately linear M - H dependence in the hard direction. The remanence versus field angle ($M_r - \phi_H$) curves of all samples show the expected behavior of in-plane uniaxial anisotropy, described by $M_r(\phi_H) = M_r(\phi_{\text{easy}}) |\cos(\phi_H - \phi_{\text{easy}})|$, where ϕ_{easy} is the direction of (the in-plane component of) the magnetic easy axis. Figure 2 shows hysteresis loops along both easy and hard directions and typical $M_r - \phi_H$ curves of LSMO films on both NGO (100)_o and NGO (001)_o. The magnetic easy and hard axes are found to be along in-plane NGO-crystal directions. For LSMO films on NGO (110)_o and NGO (010)_o the easy and hard directions are aligned with the in-plane NGO-crystal directions as well. For the films on NGO (112)_o it is found that the easy axis rotates away from the $[\bar{1}\bar{1}1]_o$ direction with increasing film thickness. This is presented in detail elsewhere.¹⁹ A summary of the easy and hard axis directions is given in Table III. We do not observe any influence of the surface steps on the magnetic anisotropy directions, as was observed earlier for LSMO on STO (001)_c.⁴ We repeated the experiments at low temperature (150 K) and found no changes in the easy and hard directions. Temperature-dependent saturation magnetization measurements follow closely the Brillouin-functional dependence for a Weiss ferromagnet with $T_C \geq 350 \text{ K}$ and a low-temperature saturation magnetization which is approximately equal to $3.5\mu_B/\text{Mn}$.

IV. DISCUSSION

From the XRD measurements it is concluded that LSMO thin films grow coherently on the five different NGO substrate surfaces, discussed here. Due to the lattice mismatch the LSMO pseudocube is deformed, creating different strain values in the different in-plane crystal directions. For all films a strong in-plane uniaxial anisotropy is found, which dominates any other anisotropies, e.g., the biaxial magneto-crystalline anisotropy and surface-step-induced anisotropy. It is evident that this anisotropy is due to the in-plane anisotropic strain in the films induced by the substrate. In general the magnetoelastic energy due to the inverse magnetostrictive effect can be described with the formula²⁰ $E_i = -\frac{3}{2}\lambda_{100}\sigma_i(\alpha_1^2\gamma_{i1}^2 + \alpha_2^2\gamma_{i2}^2) - 3\lambda_{111}\sigma_i(\alpha_1\alpha_2\gamma_{i1}\gamma_{i2})$, assuming that the magnetization is predominantly in the plane of the film. Here α_j and γ_{ij} are the direction cosines of the magnetization and the stress σ_i with the pseudocubic lattice vectors. λ_{100} and λ_{111} are the magnetostriction in the $[100]_{pc}$ and $[111]_{pc}$ directions, respectively. For uniaxial anisotropy the in-plane anisotropy easy direction is determined by the lowest energy state. To account for the case of compressive strain ε_1 in one in-plane direction, tensile strain ε_2 in the orthogonal in-plane direction, and resulting out-of-plane strain ε_3 , the energy for a given in-plane magnetization direction is written as being due to the superposition of the two strain states, $E_{\text{easy,hard}} = E_1(\sigma_1) + E_2(\sigma_2)$. [The energy due to the out-of-plane strain equals zero, $E_3(\sigma_3) = 0$, for in-plane magnetization.] In this way the sign of $\vec{\sigma}_i = Y\vec{\varepsilon}_i$ is taken into account straightforwardly. The calculated anisotropy directions are given in Table III using (the room-temperature values) $\lambda \approx 1.3$

TABLE II. Pseudocubic lattice parameters of LSMO, grown on NGO with different surface-plane orientations, as determined from XRD measurements. The in-plane lattice parameters are equal to those of the corresponding substrate lattice parameters. The error in the length is 0.005 Å and the error in the angle is 0.1°.

LSMO pseudocube lattice parameters	Length (Å)	LSMO pseudocube angles	Angle (deg)
LSMO (001) _{pc} on NGO (110) _o			
$a=c_{\text{NGO}}/2$ (in plane)	3.85	α	89.6
$b=1/2\sqrt{a_{\text{NGO}}^2+b_{\text{NGO}}^2}$ (in plane)	3.86	β	90
c (out of plane)	3.91	γ	90
LSMO (001) _{pc} on NGO (001) _o			
$a=1/2\sqrt{a_{\text{NGO}}^2+b_{\text{NGO}}^2}$ (in plane)	3.86	α	90
$b=1/2\sqrt{a_{\text{NGO}}^2+b_{\text{NGO}}^2}$ (in plane)	3.86	β	90
c (out of plane)	3.91	γ	89.3
LSMO (011) _{pc} on NGO (100) _o			
$a=c_{\text{NGO}}/2$ (in plane)	3.85	α	89.9
b	3.89	β	90
c	3.89	γ	90
$ (\mathbf{b}-\mathbf{c}) =b_{\text{NGO}}$ (in plane)	5.50	$\angle[\mathbf{a},(\mathbf{b}-\mathbf{c})]$	90
$ (\mathbf{b}+\mathbf{c}) $ (out of plane)	5.51	$\angle[\mathbf{a},(\mathbf{b}+\mathbf{c})]$	90
		$\angle[(\mathbf{b}-\mathbf{c}),(\mathbf{b}+\mathbf{c})]$	90
LSMO (011) _{pc} on NGO (010) _o			
$a=c_{\text{NGO}}/2$ (in plane)	3.85	α	88.7
b	3.88	β	90
c	3.88	γ	90
$ (\mathbf{b}-\mathbf{c}) =a_{\text{NGO}}$ (in plane)	5.43	$\angle[\mathbf{a},(\mathbf{b}-\mathbf{c})]$	90
$ (\mathbf{b}+\mathbf{c}) $ (out of plane)	5.55	$\angle[\mathbf{a},(\mathbf{b}+\mathbf{c})]$	90
		$\angle[(\mathbf{b}-\mathbf{c}),(\mathbf{b}+\mathbf{c})]$	90
LSMO (011) _{pc} on NGO (112) _o			
$a=1/2\sqrt{a_{\text{NGO}}^2+b_{\text{NGO}}^2}$ (in plane)	3.86	α	89.4
b	3.88	β	89.6
c	3.88	γ	89.6
$ (\mathbf{b}-\mathbf{c}) = \sqrt{\left(\frac{a_{\text{NGO}}}{2}\right)^2 + \left(\frac{b_{\text{NGO}}}{2}\right)^2 + (c_{\text{NGO}})^2}$ (in plane)	5.46	$\angle[\mathbf{a},(\mathbf{b}-\mathbf{c})]$	89.5
$ (\mathbf{b}+\mathbf{c}) $ (out of plane)	5.52	$\angle[\mathbf{a},(\mathbf{b}+\mathbf{c})]$	90
		$\angle[(\mathbf{b}-\mathbf{c}),(\mathbf{b}+\mathbf{c})]$	90

$\times 10^{-5}$ (Refs. 21 and 22) and $Y=1.3 \times 10^{11}$ N/m²,²³ obtained from magnetostriction and elasticity measurements on LSMO. It is assumed that $\lambda_{100}=\lambda_{111}=\lambda$. For all cases we find complete correspondence with the experimentally determined easy axis directions, except for the case of NGO (112)_o. The in-plane easy axis is in the in-plane direction with (largest) tensile strain or in the case that both strain directions are compressive, in the direction with smallest compressive strain. Earlier reports ascribe the occurrence of in plane (out-of-plane magnetization) [for example, in the case of LSMO on STO (001) and LAO (001), respectively]

as being due to the in-plane tensile (compressive strain). The resulting deformation of the oxygen octahedra surrounding the Mn, being compressed (extended) in the out-of-plane direction, should then be the cause for the anisotropy. In the cases presented here the in-plane strain is unequal in both orthogonal directions giving rise to a further in-plane deformation of the octahedra, causing the uniaxial in-plane anisotropy.

The easy axis direction in the case of LSMO/NGO (112)_o is not described correctly. We ascribe this to the strong distortions of the pseudocube, changing the angles between all

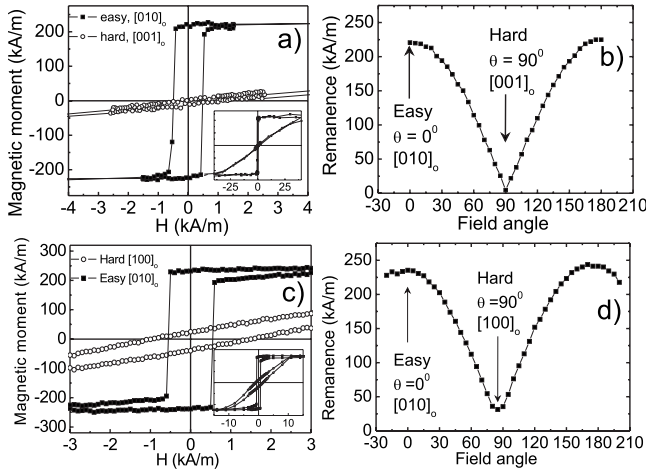


FIG. 2. Top panel: (a) hysteresis loops of a 14-nm-thick LSMO/NGO (100)_o film along in-plane easy and hard directions. (b) Remanence vs in-plane field angle for this film at room temperature. Arrows denote easy and hard directions. Bottom panel: (c) hysteresis loops of a 25-nm-thick LSMO film grown on NGO (001)_o along in-plane easy and hard directions. (d) Remanence vs in-plane field angle at room temperature. Arrows denote easy and hard directions.

pseudocube axes, whereas in the other cases most angles are orthogonal. This further reduction in the symmetry of the unit cell is clearly important for the anisotropy and is not taken into account in the simple model above.

We find a significant discrepancy between the values for the in-plane anisotropy constants calculated from the model above and the values obtained from the magnetization loops with the integration method. We ascribe this difference to the fact that the latter method can only be used if the magnetization loop can be completely described mathematically.²⁰ For our samples this is not the case as an out-of-plane contribution of the magnetization is present as well (especially at low-field values) resulting in domain formation in the out-of-plane direction. This is concluded from magnetic-force microscopy (MFM) measurements showing out-of-plane mag-

netic domains and angle dependent coercivity measurements consistent with magnetization reversal by domain-wall motion (both not shown here). Also the inverse magnetostriction model predicts out-of-plane anisotropy, which competes with demagnetization. Both aspects, rotation of the magnetization vector out of plane and the presence of multiple domains, and the associated magnetization reversal by domain-wall motion prohibit the use of the integration method²⁰ here. Even though the model cannot be used to calculate the uniaxial-anisotropy constant, it is successful in describing the easy axis directions. This is because the in-plane easy axis directions depend only on the sign of the energy difference between the in-plane magnetization in two orthogonal directions while the anisotropy constant cannot be determined without taking the energy of the out-of-plane component of the magnetization into account.

V. CONCLUSIONS

We have grown successfully epitaxial (001)_{pc}- and (011)_{pc}-oriented LSMO thin films on different NGO substrates. The LSMO growth orientation and crystal structure depends on the crystal orientation of the substrate surface plane. The films have strong in-plane uniaxial anisotropy with the easy axis directions related to the crystal directions of the substrate. The easy axis directions are explained by magnetostriction induced by the anisotropic in-plane strain. (011)_{pc}-oriented LSMO films grown on NGO may have advantages over common (001)_{pc} films when they are used as electrodes in MTJs since they combine strong uniaxial anisotropy with a surface termination that allows interfaces without interfacial charge transfer.

ACKNOWLEDGMENTS

We acknowledge financial support from NanoNed, the nanotechnology network in the Netherlands, the Dutch Technology Foundation (STW), the Netherlands Organization for Scientific Research (NWO), and the EU program NanOxide.

TABLE III. Magnetic easy and hard axes for LSMO grown on NGO. For LSMO films on NGO (112)_o the anisotropy is uniaxial, but the easy and hard axes are not aligned with the NGO-crystal directions (Ref. 19). The model easy and hard directions have been derived from the inverse magnetostrictive effect.

	In-plane direction	Lattice mismatch (%)		Expt.	Model
LSMO (001) _{pc} on NGO (110) _o	[1 $\bar{1}$ 0] _o	-0.47		Easy	Easy
	[001] _o	-0.70		Hard	Hard
LSMO (001) _{pc} on NGO (001) _o	[100] _o	-1.11		Hard	Hard
	[010] _o	+0.16		Easy	Easy
LSMO (011) _{pc} on NGO (100) _o	[010] _o	+0.16		Easy	Easy
	[001] _o	-0.70		Hard	Hard
LSMO (011) _{pc} on NGO (010) _o	[100] _o	-1.11		Hard	Hard
	[001] _o	-0.70		Easy	Easy
LSMO (011) _{pc} on NGO (112) _o	[$\bar{1}$ 10] _o	-0.47		Approximately hard	Easy
	[$\bar{1}$ 11] _o	-0.59		Approximately easy	Hard

*j.a.boschker@utwente.nl

†e.p.houwman@utwente.nl

- ¹J.-H. Park, E. Vescovo, H. J. Kim, C. Kwon, R. Ramesh, and T. Venkatesan, *Nature (London)* **392**, 794 (1998).
- ²M. Bowen, M. Bibes, A. Barthélémy, J. P. Contour, A. Anane, Y. Lemaitre, and A. Fert, *Appl. Phys. Lett.* **82**, 233 (2003).
- ³J. M. De Teresa, A. Barthélémy, A. Fert, J. P. Contour, R. Lyonnet, F. Montaigne, P. Seneor, and A. Vaurès, *Phys. Rev. Lett.* **82**, 4288 (1999).
- ⁴M. Mathews, F. M. Postma, J. C. Lodder, R. Jansen, G. Rijnders, and D. H. A. Blank, *Appl. Phys. Lett.* **87**, 242507 (2005).
- ⁵K. Steenbeck and R. Hiergeist, *Appl. Phys. Lett.* **75**, 1778 (1999).
- ⁶Z. H. Wang, G. Cristiani, and H. U. Habermeier, *Appl. Phys. Lett.* **82**, 3731 (2003).
- ⁷E. P. Houwman, G. Maris, G. M. De Luca, N. Niermann, G. Rijnders, D. H. A. Blank, and S. Speller, *Phys. Rev. B* **77**, 184412 (2008).
- ⁸Y. Mukunoki, N. Nakagawa, T. Susaki, and H. Y. Hwang, *Appl. Phys. Lett.* **86**, 171908 (2005).
- ⁹I. C. Infante, F. Sanchez, J. Fontcuberta, S. Fusil, K. Bouzehouane, G. Herranz, A. Barthelemy, S. Estrade, J. Arbiol, F. Peiro, R. J. O. Mossaneck, M. Abbate, and M. Wojcik, *J. Appl. Phys.* **101**, 093902 (2007).
- ¹⁰P. Lecoeur, P. L. Trouilloud, G. Xiao, A. Gupta, G. Q. Gong, and X. W. Li, *J. Appl. Phys.* **82**, 3934 (1997).
- ¹¹C. Kwon, M. C. Robson, K.-C. Kim, J. Y. Gu, S. E. Lofland, S. M. Bhagat, Z. Trajanovic, M. Rajeswari, T. Venkatesan, A. R. Kratz, and R. Ramesh, *J. Magn. Magn. Mater.* **172**, 229 (1997).
- ¹²Joonghoe Dho, Y. N. Kwo, Y. S. Hwang, J. C. Kim, and N. H. Hur, *Appl. Phys. Lett.* **82**, 1434 (2003).
- ¹³F. Tsui, M. C. Smoak, T. K. Nath, and C. B. Eom, *Appl. Phys. Lett.* **76**, 2421 (2000).
- ¹⁴L. A. Vasylechko, W. Morgenroth, U. Bismayer, A. Matkovskii, and D. Savvitskii, *J. Alloys Compd.* **297**, 46 (2000).
- ¹⁵M. Mathews, Ph.D. thesis, University of Twente, 2007.
- ¹⁶A. Vailionis, W. Siemons, and G. Koster, *Appl. Phys. Lett.* **93**, 051909 (2008).
- ¹⁷K. Steenbeck (private communication).
- ¹⁸Torque measurements have to be performed with the sample fully magnetized in the direction of the applied field, which requires a large applied field. This field induces significant magnetization in the paramagnetic substrate which dominates the measurements. For angle dependent VSM measurements, however, the main information about the anisotropy is obtained from the remanence in the magnetization loop where the substrate magnetization is zero.
- ¹⁹H. Nishikawa, E. P. Houwman, H. Boschker, M. Mathews, G. Rijnders, and D. H. A. Blank, *Appl. Phys. Lett.* **94**, 042502 (2009).
- ²⁰S. Chikazumi, *Physics of Magnetism* (Wiley, New York, 1964).
- ²¹N. Zhang, X.-M. Yin, M. Wang, T. Schneider, and G. Srinivasan, *Chin. Phys. Lett.* **23**, 463 (2006).
- ²²R. V. Demin, L. I. Koroleva, and A. M. Balbashov, *J. Magn. Magn. Mater.* **177–181**, 871 (1998).
- ²³V. Rajendran, S. Muthu Kumuran, V. Sivasubramanian, T. Jayakumar, and B. Raj, *Phys. Status Solidi A* **195**, 350 (2003).